Journal of the Earth and Space Physics
Homepage: https://jesphys.ut.ac.ir
Vol. 51, No. 4, Winter 2026, P. 89-103
(Research Article)

Spatial-Temporal Variations and Trends in Freezing Level Height in Iran: An Analytical Perspective

Ghadermazi, H.[1] | Masoompour Samakosh, J.[1] ✉ | Fatemi, S. E.[2] | Hafezparast, M.[2]

1. Department of Geography, Faculty of Literature and Humanities, Razi University, Kermanshah, Iran.
2. Department of Water Engineering, Campus of Agriculture and Natural Resources, Razi University, Kermanshah, Iran.

Corresponding Author E-mail: j.masoompour@razi.ac.ir

(Received: 16 Dec 2024, Revised: 5 Jan 2025, Accepted: 29 April 2025, Published online: 17 March 2026)

Abstract

This research investigates the temporal and spatial changes of freezing level height (FLH) in Iran over the statistical period from 1940 to 2023, using the modified Mann-Kendall non-parametric analysis method. The results indicate a significant upward trend in FLH from December to April. Except for summer, the upward trend is quite evident during autumn, winter, and spring. Annual changes in FLH show a significant upward trend during the study period. These significant upward trends at monthly, seasonal, and annual scale can show one of the consequences of climate change in Iran. Spatial analysis reveals an inverse relationship with the latitude, and as latitude decreases (towards southern regions of Iran), FLH increases. This relationship is more clear in winter, with the correlation coefficient between FLH and latitude being significant at the 0.05 alpha level. Additionally, FLH shows a direct relationship with longitude, increasing as one moves eastward. The highest freezing level height is observed in Chabahar (4347.5 meters) in southeastern Iran. Considering the decrease in snow cover and increase in heavy rainfall in Iran, monitoring variations in freezing level height can be useful for predicting these variables.

Keywords: Freezing Level Height, Trend, Sen's slop, Iran.

1. Introduction

The freezing level height (FLH) is the altitude at which the air temperature is 0°C (the isotherm), indicating the approximate location of the phase transition of water between solid and liquid, as well as sublimation from solid to vapor. FLH is a critical parameter for understanding hydrological conditions and climate change (Guo et al., 2021).

At levels above the freezing height, the air temperature is below zero degrees Celsius, while at lower levels, the temperature is above zero degrees Celsius. The height of the freezing level, or the zero-degree isotherm in the atmosphere, is a parameter that determines the ice cover of mountains and high areas with the change of water to ice (Harris et al., 2000; Vuille et al., 2004; Coudrain et al., 2005; Vuille et al., 2008).

The height of the freezing level in high mountain areas is an essential parameter in the durability and extent of snow and ice cover, playing a prominent role in both melting and freezing. This parameter also affects the amount and status of water resources (Diaz and Graham, 1996; Harris et al., 2000; Diaz et al., 2003; Bradley et al., 2009; Folkins, 2013).

Unfortunately, climate and hydrological research in the cryosphere is limited by the lack of sufficient climate data from icy and high mountain areas. Considering the mentioned obstacles, the FLH survey obtained from radiosonde data or network data, can provide more accurate information to detect changes in the cryosphere, the extent of snow cover, and its response to climate change. In addition, with low FLH in the atmosphere and strong updrafts, hail formation is enhanced (Dessens, 1986). On the other hand, data limitations prevent a detailed examination of seasonal and monthly trends (Khansalari, 2020).

Previous research indicates that the height of the freezing level has been rising globally since the late 1950s, particularly in tropical and especially in extratropical regions. This increase in temperature has had a significant

Cite this article: Ghadermazi, H., Masoompour Samakosh, J., Fatemi, S. E., & Hafezparast, M., (2026). Spatial-Temporal Variations and Trends in Freezing Level Height in Iran: An Analytical Perspective. *Journal of the Earth and Space Physics*, 51(4), 89-103. DOI: http//doi.org/10.22059/jesphys.2025.386947.1007650

E-mail: (1) hasan.ghadermazi@gmail.com (2) se.fatemi92@gmail.com | maryam.hafezparast2@gmail.com

Publisher: University of Tehran Press.
DOI: http//doi.org/10.22059/jesphys.2025.386947.1007650
Print ISSN: 2538-371X
Online ISSN: 2538-3906

impact on the conditions of the cryosphere and snowy mountain areas (Diaz and Graham, 1996; Gaffen et al., 2000; Harris et al., 2000; Diaz et al., 2003; Seidel and Free, 2003; Bradley et al., 2009). The rate of temperature increase has caused FLH to increase with increasing altitude. This phenomenon is significantly more severe in mountainous regions (Diaz et al., 2014; Pepin et al., 2015). Recent studies in China clearly show, on a regional scale, the warming of both land surface temperature and tropospheric air temperature, along with an increase in FLH since the 1960s (Zhang and Guo, 2011; Chen et al., 2012; Dong et al., 2012; Huang et al., 2013; Wang et al., 2014; Zhang et al., 2014a; Zhang et al., 2014b).

Since the freezing level height is closely related to rain and snow depth, it is important to study its changes and how it is associated with the type of precipitation and cold waves and frost, especially in mountainous areas. It is also an essential parameter for changes in the cryosphere, as it indicates the approximate location of permanent ice and snow on the Earth's surface. Therefore, the freezing level is an important indicator of climate variability and change. Considering these cases, it is necessary to conduct comprehensive and detailed studies of the freezing level height in Iran, a country characterized by diverse climatic regions and complex topography, which is also important in determining the status of water resources.

2. Methods

2.1. The study area

Iran is one of the largest countries in the world, located between 25°3' and 39°47' north latitude and 44°5' and 63°18' east longitude and in the Middle East region as well as the vicinity of Central Asia and the Caucasus (Figure 1). Due to its geographical location, which has changes in altitude, distance from the sea, wideness and long distance between north and south, which covers from latitude 25 degrees to 40 degrees north, Iran experiences a very diverse climate. Therefore, the humidity conditions in this land vary from very dry to very humid. The amount of rainfall fluctuates in different regions of the country and varies significantly from year to year.

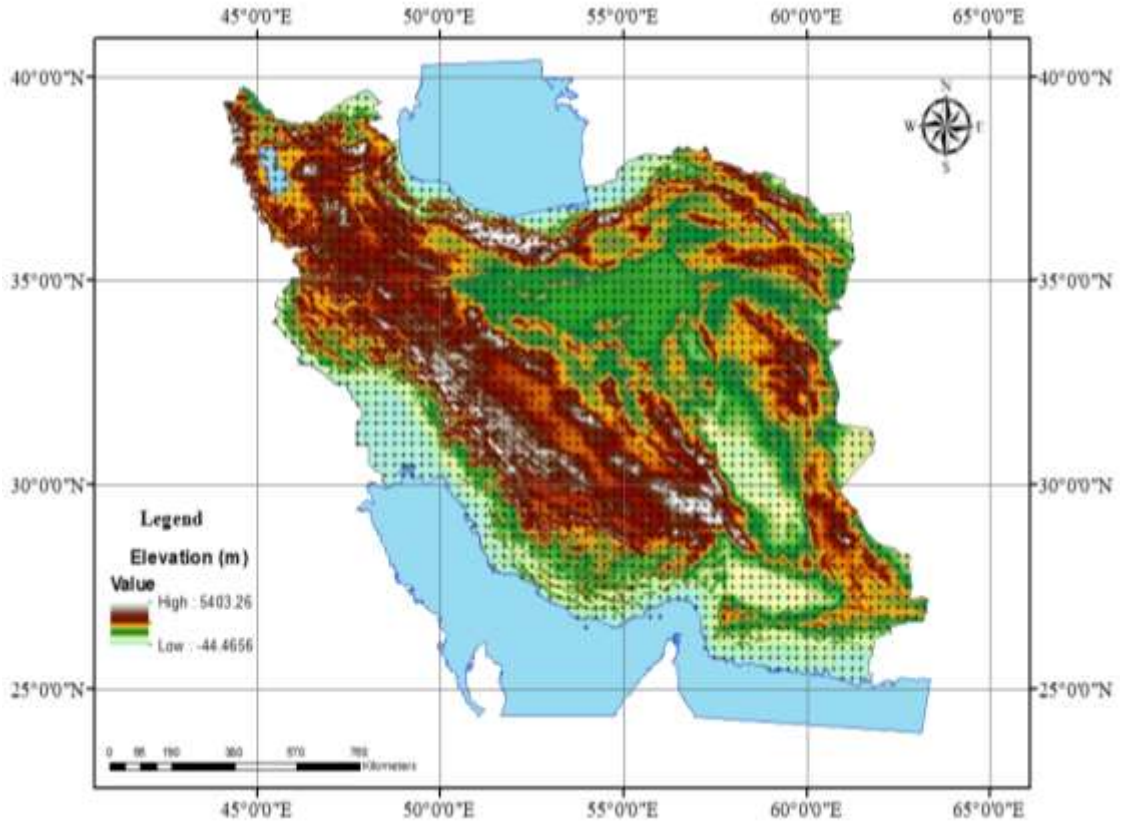

Figure 1. Geographical location of Iran and spatial distribution of network data, 0.25 * 0.25.

2-2. Data

In this study, average raster data of the freezing level with a resolution of 0.25 x 0.25 in 12 hours of every month from 1940 to 2023 have been used. The data were obtained from the climatic database of the European Centre for Medium-Range Weather Forecasts (ECMWF). The selected range includes from 44 Degrees east longitude to 64 Degrees east longitude and from 23 Degrees north latitude to 44 Degrees north latitude (the location of Iran). For statistical analysis, network data were converted into vector data in GIS software, and level maps of freezing level were extracted. The statistical parameters of the monthly freezing level from 1940 to 2023 are shown in Table 1. According to Table 1, the average FLH is at the lowest altitude (1347 m) in January and the highest altitude (4145.8 m) in July.

2-3. Methods

Monthly maps of freezing level elevation (1009 months) were extracted for trend analysis. Then, the maps of the same months were arranged as time series for each twelve months, and the trend of changes in these monthly time series were analyzed using the modified nonparametric Mann-Kendall test.

One conventional method in the analysis of climate data time series is to examine the presence or absence of trends caused by gradual natural changes and climate changes caused by human activities (Liu et al., 2020). The nonparametric Mann-Kendall test, as a suitable method for proving the existence of trends in climate series, has been used in recent years as the best option for examining seasonal and annual changes in climate variables such as temperature and precipitation (Lornezhad et al., 2023). The Mann-Kendall method was first proposed by Mann (1945) and later extended and developed by Kendall (1970). The null hypothesis of the Mann-Kendall test indicates the randomness and the absence of a trend in the data series, and accepting the one hypothesis (rejection of the null hypothesis) suggests the presence of a trend in the data series (Sen, 1968).

2-3-1. Mann-Kendall Test (MK)

The Mann—Kendall (MK) analysis uses non-parametric trend development only for reliable data. It has been generally practical where the data are not identical to a normal distribution (non-parametric). The Mann-Kendall test is used globally to analyze trends in meteorological variables (Tabari et al., 2015). World Metrological Data have been widely suggested for this test and are freely available to the public to assess trends (Shi et al., 2013) and to detect the statistically significant trends in long-term data. Two hypothesis tests must be tested in the MK, Null hypothesis and, Alternative Hypothesis. The null hypothesis defines the absence of a trend in the time series of data, while the alternative hypothesis states that there is a significant trend in the time series. The MK test does not require the assumption of normality, and not only indicates the direction but also the magnitude of significant trends. The Mann-Kendall test measured values (Xj-Xk), where j>k and test statistics S is computed exerting the formula.

$$S = \sum_{k=1}^{n-1} \sum_{j=k+1}^{n} sign(x_j - x_k) \quad (1)$$

where Xj and Xk are the annual values in years j and k, j>k, respectively.

$$sign(x_j - x_k) \begin{cases} 1 \ if \ (x_j - x_k) > 0 \\ 0 \ if \ (x_j - x_k) = 0 \\ -1 \ if (x_j - x_k) < 0 \end{cases} \quad (2)$$

It is necessary to compute the probability associated with S and the sample size n, to quantify the significance of the trend statistically, The calculating formula of variance S is denominating as:

$$Var(S) = \frac{[n(n-1)(2n+5) - \sum_{p=1}^{q} t_p(t_p-1)(2t_p+5)]}{18} \quad (3)$$

Where q is defined as the number of tied groups and tp is the number of data in the pth group. The values of S and VAR(S) are accustomed to calculate the test statistics Z, which is following as;

$$Z = \begin{cases} \frac{s-1}{\sqrt{Var(s)}} & if \ S > 0 \\ 0 & if \ S = 0 \\ \frac{s+1}{\sqrt{Var(s)}} & if \ S < 0 \end{cases} \quad (4)$$

Z score follows a normal distribution. At a Level of α=0.05 (95% confidence interval) with a two-sided alternative, the critical values at 0.025 are equal to -1.96 to 1.96. The trend is said to be decreasing if Z is negative and its absolute value is greater than

the level of significance, while it is increasing if Z is positive and greater than the label of significance. If n≤10 the normal approximation test is used, and a statistically significant trend is computed exerting the Z score. Mann Kendall & Sen's slope estimator test the Z score significance level at α:0-001, 0.05, and 0.1.
The test statistics τ can be computed as:

$$\tau = \frac{s}{n-(n-1)/2} \quad (5)$$

2-3-2. Mann–Kendall test with trend-free pre-whitening (TFPW)

When autocorrelation is positive or negative, there will be a decrease or increase in the value of S, which will be under- or overestimated by the original variance V(S) (Hamed, 2009). Therefore, when trend analysis conducted on this data using MK1, it will show positive or negative trends when there is no trend. Hence, the trend free pre-whiting process (TFPW) was proposed (Hamed, 2009), in which the slope and lag-1 serial correlation coefficient are estimated simultaneously. The lag-1 serial correlation coefficient is then corrected for bias before pre-whitening. Finally, the lag-1 serial correlation components are removed from the series before applying the trend test. The following steps are used to determine trend analysis using the MK2 test. Calculate the lag-1 (k = 1) autocorrelation coefficient (r1) using:
1-Calculate the lag-1 (k = 1) autocorrelation coefficient (r_1) by:

$$\boldsymbol{r_1} = \frac{\frac{1}{n-k}\sum_{i=1}^{n-k}(x_i-\bar{x})(x_{i+k}-\bar{x})}{\frac{1}{n}\sum_{i=1}^{n}(x_t-\bar{x})^2} \quad (6)$$

If $\frac{\{-1-1.96\sqrt{n-2}\}}{n-1} \le \boldsymbol{r_1} \le \frac{\{-1+1.96\sqrt{n-2}\}}{n-1}$ is satisfied, then the series is assumed to be independent at a 5% significance level and there is no need for pre-whitening.
Otherwise, pre-whitening is required for the series before applying the MK1 test.
Equation (7) is used to remove the trend in time series

$$X'_i = X_i - (\beta \times i) \quad (7)$$

Data to get a detrended time series.
Where

$$\beta = Median = \left[\frac{x_j - x_i}{j-i}\right] (\forall j > i) \quad (8)$$

Using Equation (9), remove the lag-1 autoregressive component (AR (1)) from the detrended series to get a residual series as fallow;

$$Y'_i = X'_i - r1 * X'_{i-1} \quad (9)$$

Thus, the MK test is applied to the blended series Yi to determine the significance of the trend.

2-3-4. Modified Mann-Kendall test with variance correction (MMK)

Sometimes, removing lag-1 autocorrelation is insufficient for many Hydroclimatologic time series datasets. A correction procedure was proposed by (Hamed and Rao, 1998) to overcome the limitation of serial autocorrelation in time series. First, the corrected variance S is calculated using Equation (10), where V (S) is the variance of the MK1, and CF is the correction factor due to the existence of serial correlation in the data. The corrected variance is given by:

$$S\big(V \times (s)\big) = CF \times V(S) \quad (10)$$

Where

$$CF = 1 + \frac{2}{n(n-1)9n-2)}\sum_{k=1}^{n-1}(n-k)(n-k-1)(n-k-2)r_k^R \quad (11)$$

where r_k^R is lag-ranked serial correlation, while n is the total number of observations. The advantage of the MK3 test over the MK2 test is that it includes all possible serial correlations (lag-k) in the time series, at the same time MK2 only considers the lag-1 serial correlation (Yue et al., 2002).

2-3-5. Sen's Slope Estimator

Sen (1968) presented a non-parametric method for time series analysis by developing and expanding a series of statistical studies conducted by Thiel (1950). Similar to the Mann-Kendall method, this approach analyzes the differences between observations in a time series. Also, this test can be easily used when there are missing data. This method is based on calculating the median slope of the time series and judging the significance of the obtained slope at different confidence levels (Khorshiddoust et al., 2018). In this case, linear model f(t) can be denominated as:

$$f(t) = Q_t + B \quad (12)$$

where Q is the slope, B is constant. According to Pohlert (2016), initially, a set of linear slopes is calculated as follows (Equation 13):

$$Q_i = \frac{x_j - x_k}{j-k}. i = 1.2.3. \ldots N. j > k \quad (13)$$

If there are n values Xj in the time series, there will be as many as N=n (n1)/2 slope estimate Qi.

3. Results and discussion

The results of the monthly analysis of freezing level height in Iran show that fluctuations in the freezing level are different during the months of the year (Table 1). The freezing level height ranges from December to March fluctuates from the ground level (zero level) to the height of 5894.1m during August. The highest fluctuation in freezing level height is observed in November (4966.5 m), and the lowest fluctuation is observed during July (3654.5 m). Monthly changes in freezing level elevation and data distribution relative to the mean for each month are shown (Figure 2).

Table1. Statistical parameters of the monthly FLH-(1940-2023).

Monthly	Absolute Max	Average	Absolute Min	Range	Sd	CV%
Jan	4347.5	1347.0	0.0	4347.5	173.4	12.9
Feb	4562.4	1486.0	0.0	4562.4	189.3	12.7
Mar	4654.1	1902.9	0.0	4654.1	196.4	10.3
Apr	5138.1	2537.0	226.5	4911.6	201.4	7.9
May	5458.8	3149.0	660.9	4797.9	166.4	5.3
Jun	5679.0	3790.9	1379.0	4300.0	149.0	3.9
Jul	5637.9	4145.8	1983.4	3654.5	147.6	3.6
Aug	5894.1	4017.4	1858.2	4035.9	147.9	3.7
Sep	5583.1	3610.8	1449.6	4133.5	148.3	4.1
Oct	5435.4	2935.8	40.2	5395.2	234.7	8.0
Nov	4997.9	2221.1	31.4	4966.5	211.4	9.5
Dec	4823.3	1666.2	0.0	4823.3	217.3	13.0
Season's average	**Max**	**Average**	**Min**	**Range**	**Sd**	**%CV**
Winter	2033.1	1576.7	1168.5	864.6	182.1	11.5
Spring	3420.6	3159.0	2858.9	561.6	122.8	3.9
Summer	4138.0	3924.7	3728.1	409.9	95.3	2.4
Autumn	2790.6	2274.3	1740.6	1049.9	158.2	7.0
Annual's average	**Max**	**Average**	**Min**	**Range**	**Sd**	**%CV**
(1940-2023)	3095.6	2733.7	2374	721.6	139.6	6.3

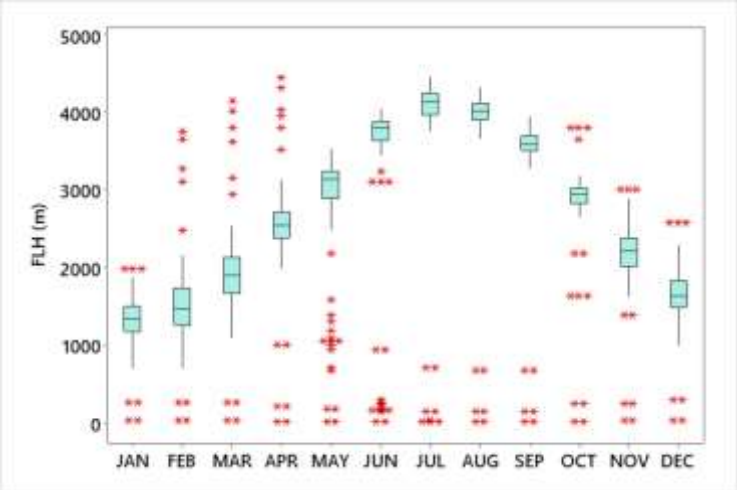

Figure 2. Boxplot of Monthly FLH (1940-2023)**.**

3-1. Monthly trend analysis

The analysis of monthly freezing surface height trends, based on the modified Mann-Kendall method, is depicted in Figure 3. The results indicate a significant upward trend in the freezing level height from December to April at the alpha level of 0.05. The trend of increasing the height of the freezing level during March and April is more intense and is significant at the alpha level of 0.01. During the summer season, there is an increase in the height of the freezing level based on the age gradient, but it is not statistically significant. Notably, there is a substantial increase in freezing level height in June. The results obtained from this study are consistent with the results of recent studies in China (Guo et al., 2021), the Andes Mountains (Mardones, 2020), and the Tibetan Plateau (Wang et al., 2014). It seems that the upward trend in increasing the height of the freezing level is in line with climate change and global warming, reflecting the consequences of climate change in the region. The monthly freezing level trend analysis results are summarized in Table 2. In Figures 3 and 4, the trend graphs of the monthly FLH and the trend slope are drawn based on the Mann-Kendall and Sen's methods.

Table 2. Monthly Mann-Kendall Trend and Sen's slope of FLH (1940-2023).

Months	Kendall's tau	p-value	Sen's slope
Jan	0.147	0.011*	2.109
Feb	0.173	0.02*	2.852
Mar	0.232	0.009**	3.454
Apr	0.305	0<0001**	3.465
May	0.102	0.195	0.887
Jun	0.15	0.017*	1.037
Jul	-0.004	0.945	-0.033
Aug	0.009	0.917	0.064
Sep	0.024	0.675	0.144
Oct	0.106	0.156	0.965
Nov	0.058	0.437	0.772
Dec	0.188	0.024*	3.367

$\boldsymbol{\alpha^{*} = 0.05, \alpha^{**} = 0.01}$

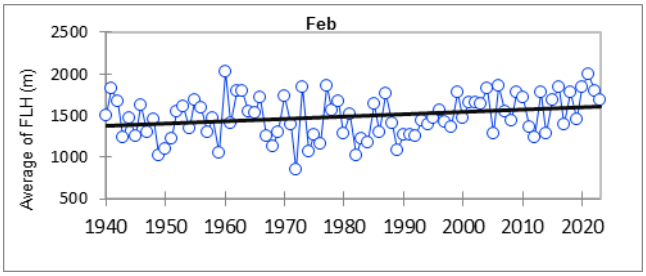

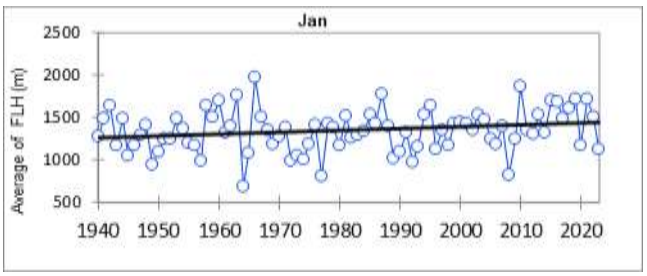

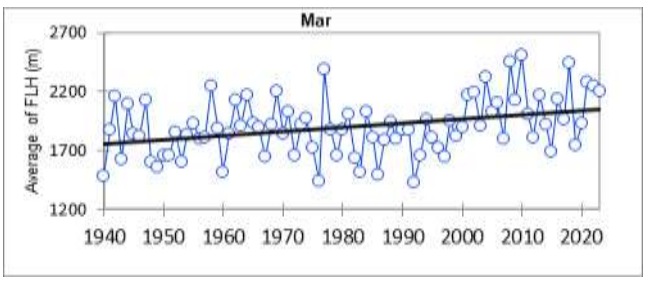

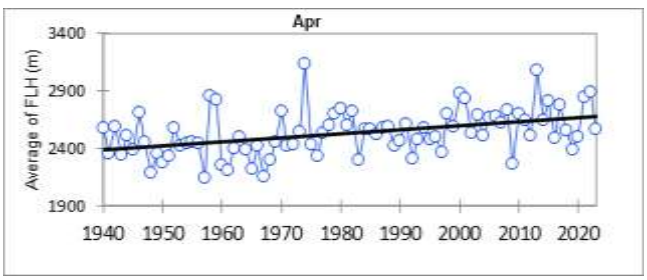

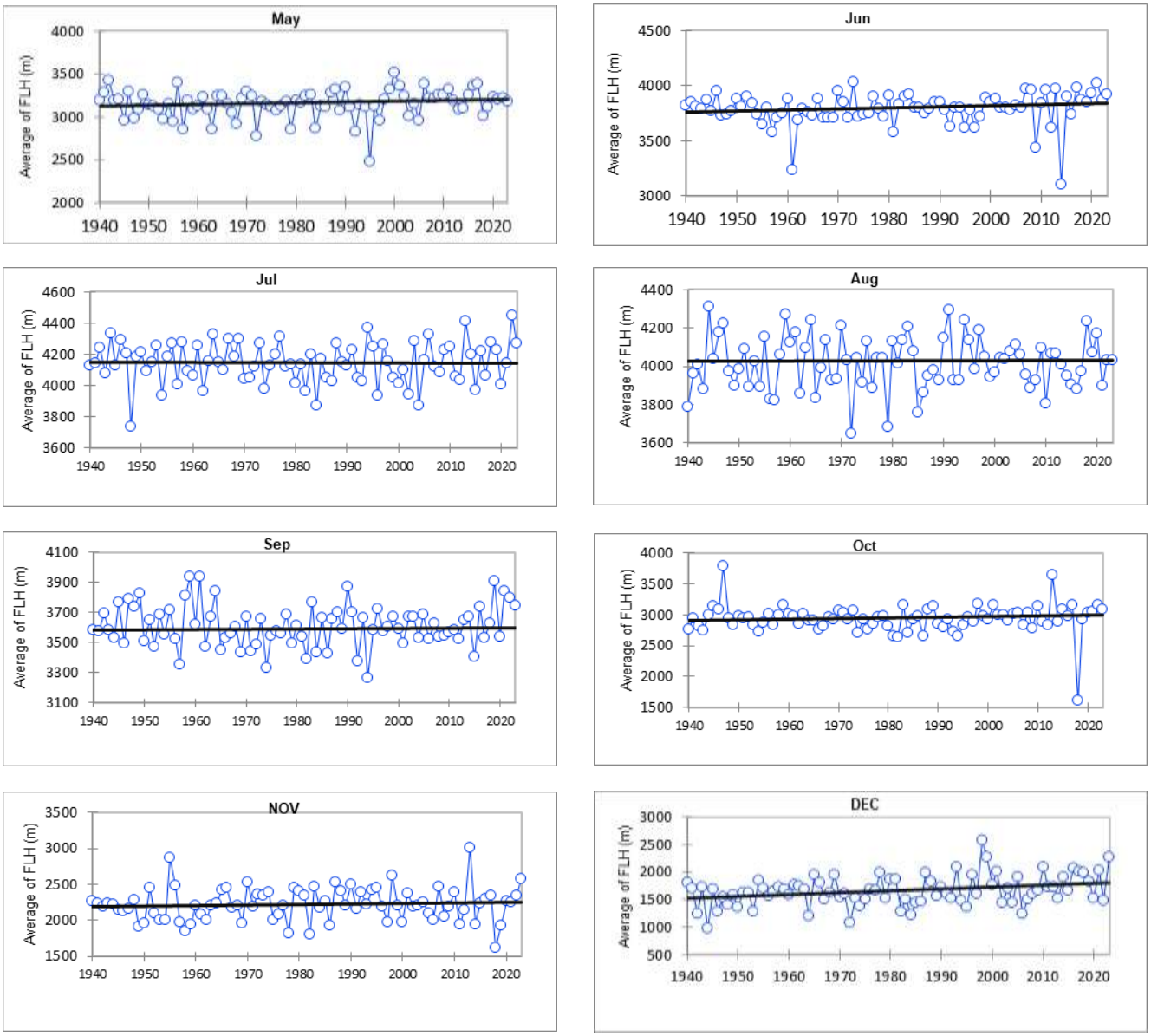

Figure 3. Mann-Kendall Trend and Sen's slope Graphs of Monthly FLH (1940-2023).

3-2. Seasonal trend analysis

The analysis results of the seasonal freezing level (Table 3 and Figure 4) show a significant increase during the winter, spring, and autumn seasons. The rate of increase in the freezing level height is higher in winter than in other seasons. This can justify the decreasing trend of snowfall in the region. Although the freezing level height in summer shows a tendency to increase, this change is not significant. These findings are consistent with studies conducted in other regions. For example, the increasing trend of FLH in China is closely related to tropospheric warming and shows clear regional and seasonal variations (Guo et al., 2021). With a more pronounced increase in northern and western China during autumn and winter, it was found that FLH in the tropical atmosphere has increased in most regions, especially in the outer tropics, with an increase in surface and upper-air temperatures of 0.1 °C per decade over the past 50 years in the tropical Andes (Bradley et al., 2009).

Table 3. Seasonal Mann-Kendall Trend and Sen's slope of FLH (1940-2023).

Months	Kendall's tau	p-value	Sen's slope
Winter	0.239	**< 0.0001****	2.698
Spring	0.241	**0.001****	1.699
Summer	0.022	0.772	0.136
Atumun	0.172	**0.008****	1.516

$\boldsymbol{\alpha^{*} = 0.05, \alpha^{**} = 0.01}$

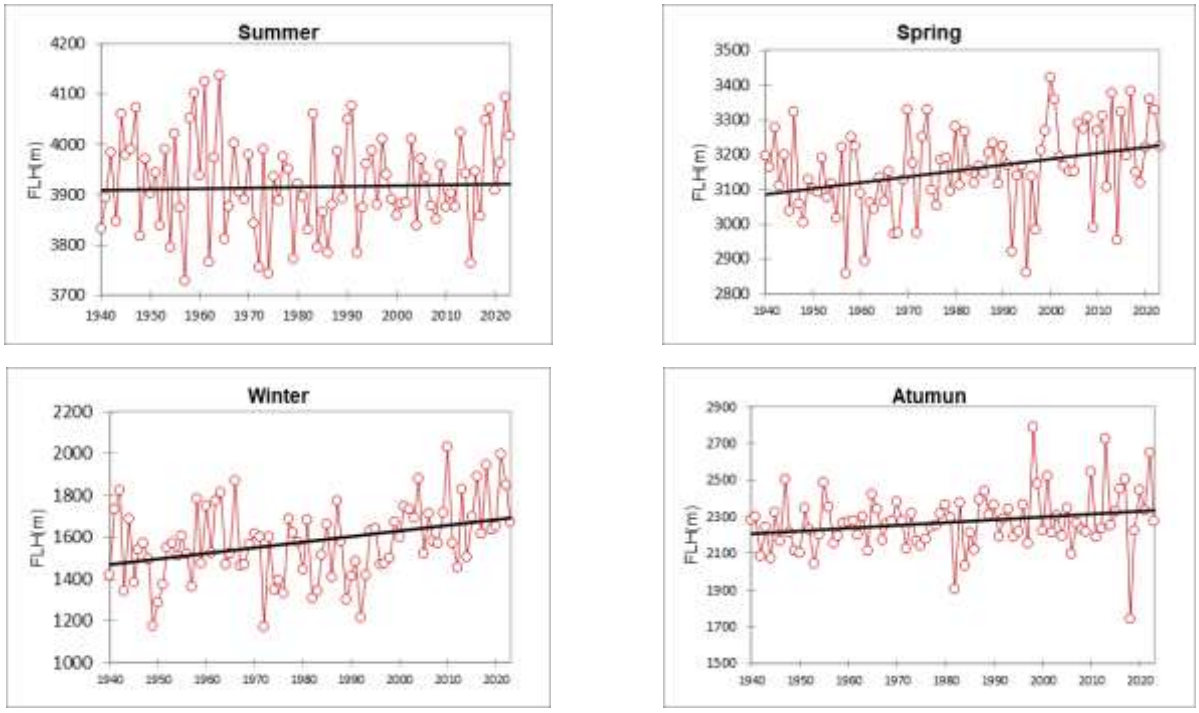

Figure 4. Mann-Kendall Trend and Sen's slope Graphs of Seasonal FLH (1940-2023)

3-3. Annual trend analysis

The annual trend analysis indicates that the height of the FLH has an increasing trend at the 0.01 alpha level of (Table 4 and Figure 5). On average, the increase in the height of the FLH is 12.2 meters per decade. The analysis of monthly, seasonal, and annual trends confirms that the increase in FLH is a consequence of global warming and climate change in the study area.

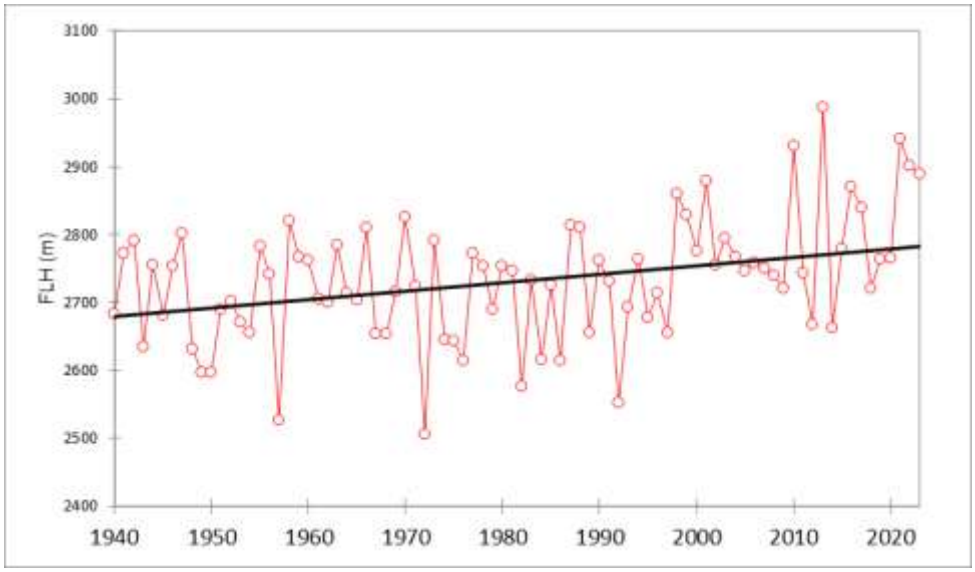

Figure 5. Mann-Kendall Trend and Sen's slope Graphs of Annual Average FLH (1940-2023).

Table 4. Annual Average Mann-Kendall Trend and Sen's slope of FLH (1940-2023).

Series	Kendall's tau	p-value	Sen's slope
Annual	0.239	**0.001****	1.241

$\boldsymbol{\alpha^{*} = 0.05, \alpha^{**} = 0.01}$

3-4. Spatial analysis

Due to the similarity in the monthly, seasonal, and annual distribution patterns of the freezing level height maps, only the spatial analysis results on seasonal and yearly scales are presented in this section. The results of examining the spatial changes show that the freezing level height has an inverse relationship with geographic latitude; and as latitude decreases (toward the southern regions of Iran), the freezing level height increases. This relationship is stronger in winter and autumn, and it weakens as the warm season approaches (Figure 6).

The correlation coefficient of the changes in FLH with latitude is significant at the 0.05 alpha level and shows that the region's latitude affects FLH. Based on the map analysis, the lowest FLH value over the entire period is observed at ALAM KOUH (52° E , 36°N) in the central Alborz in the north of Iran, while the highest freezing level is observed in the southeastern regions of the country, around Chabahar (61.5°E , 25.25°N) port (Figure 6).

The spatial distribution of the freezing level height on a seasonal scale shows that the slope of the freezing surface increases from north to south and from west to east (Figures 7 and 8).

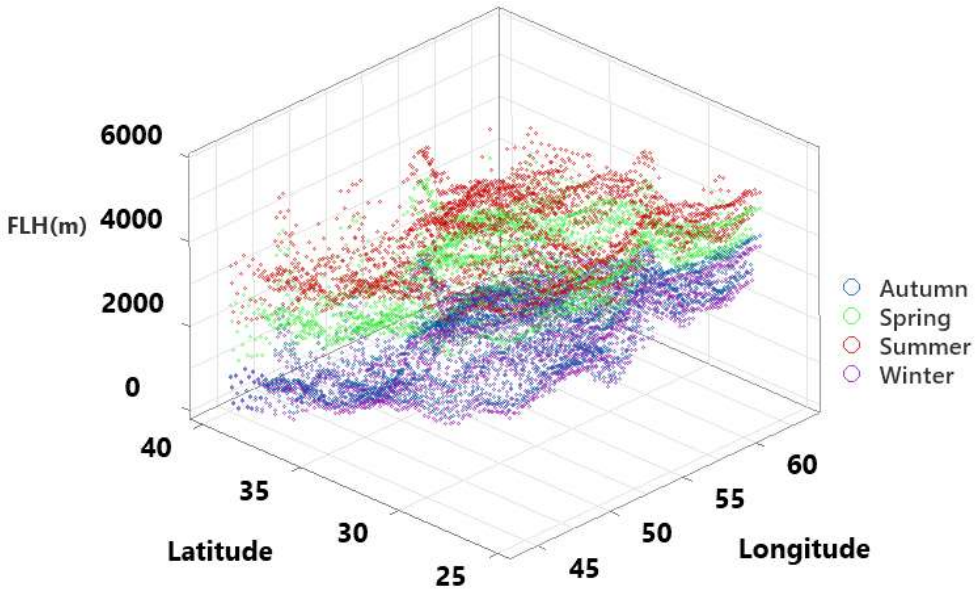

Figure 6. 3D spatial distribution of seasonal FLH in Iran (1940-2023)**.**

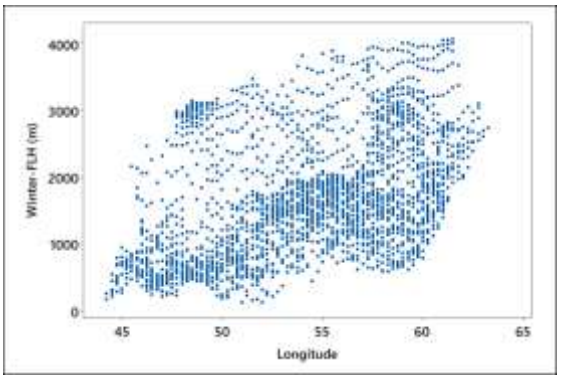

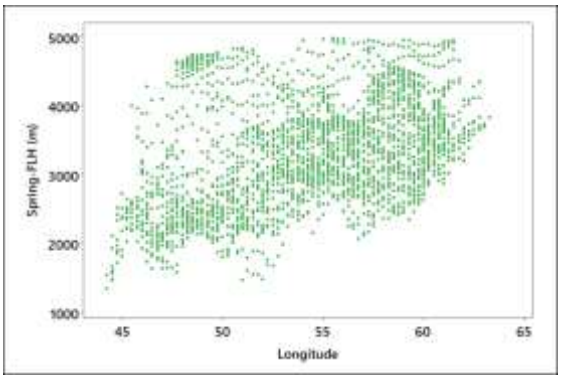

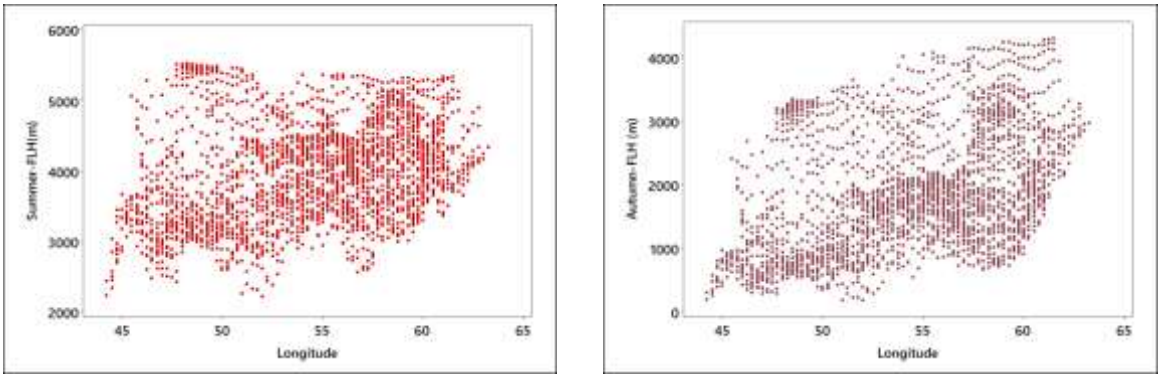

Figure 7. Seasonal spatial distribution of FLH (1940-2023) with longitude.

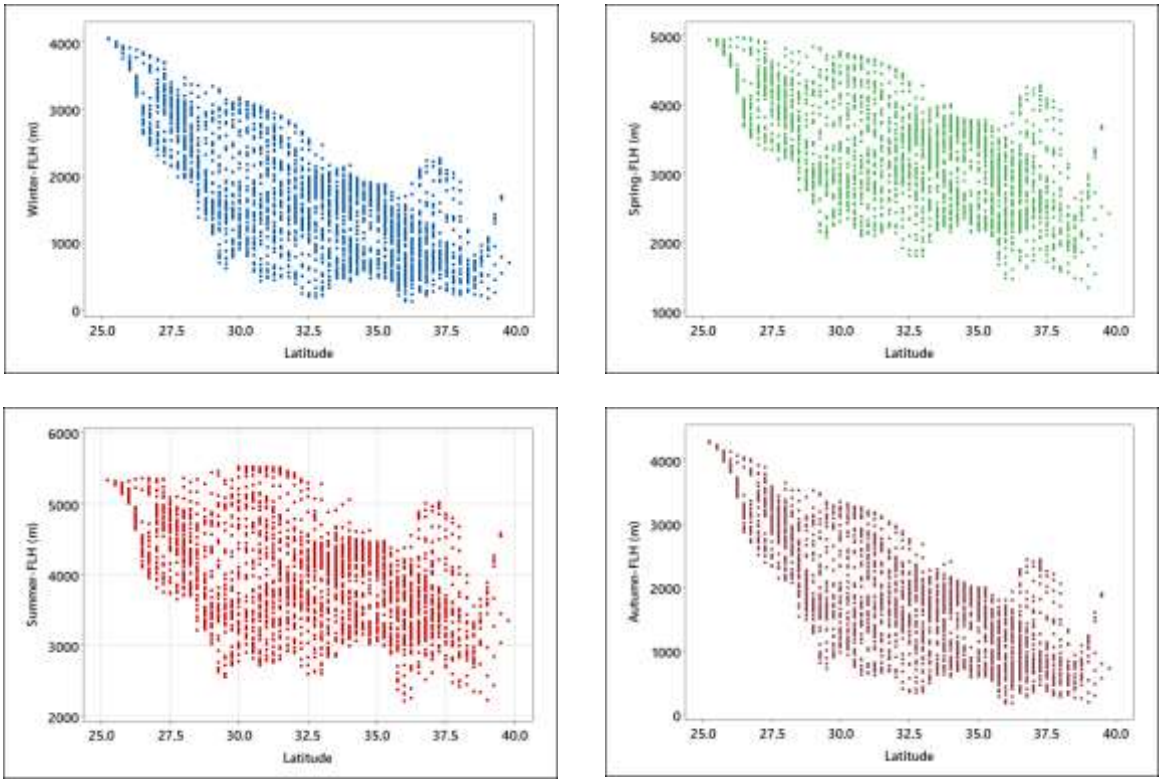

Figure 8. Seasonal spatial distribution of FLH (1940-2023) with latitude.

The relationship between the height of the freezing level and geographic longitude is direct. As we move from west to east (increasing longitude), FLH increases (Figure 9). It is clear that the western half of the country is mountainous, which has caused the temperature to decrease, resulting in a lower freezing level height.. In contrast, the eastern half of the country has lower altitude, as well as weak vegetation and bare soil causing an increase in surface temperature and naturally the freezing level rises. This can reveal the relationship between freezing level height and surface temperature. Therefore, the correlation between FLH and near-surface temperature is consistent with the results of previous studies (Diaz and Graham, 1996; Harris et al., 2000).

The value of the correlation coefficient between the height of the freezing level and latitude and longitude shows that the highest correlation value is observed in the autumn season and the lowest in the summer season (Table 4).

Table 4. The value of correlation coefficient FLH with latitude and longitude.

Season	*X*	*Y*	*P-value*
Autumn	0.4708	-0.7514	0.0000
Spring	0.4501	-0.5876	0.0000
Summer	0.3221	-0.4637	0.0000
Winter	0.4828	-0.7415	0.0000
Annual	0.4445	-0.6593	0.0000

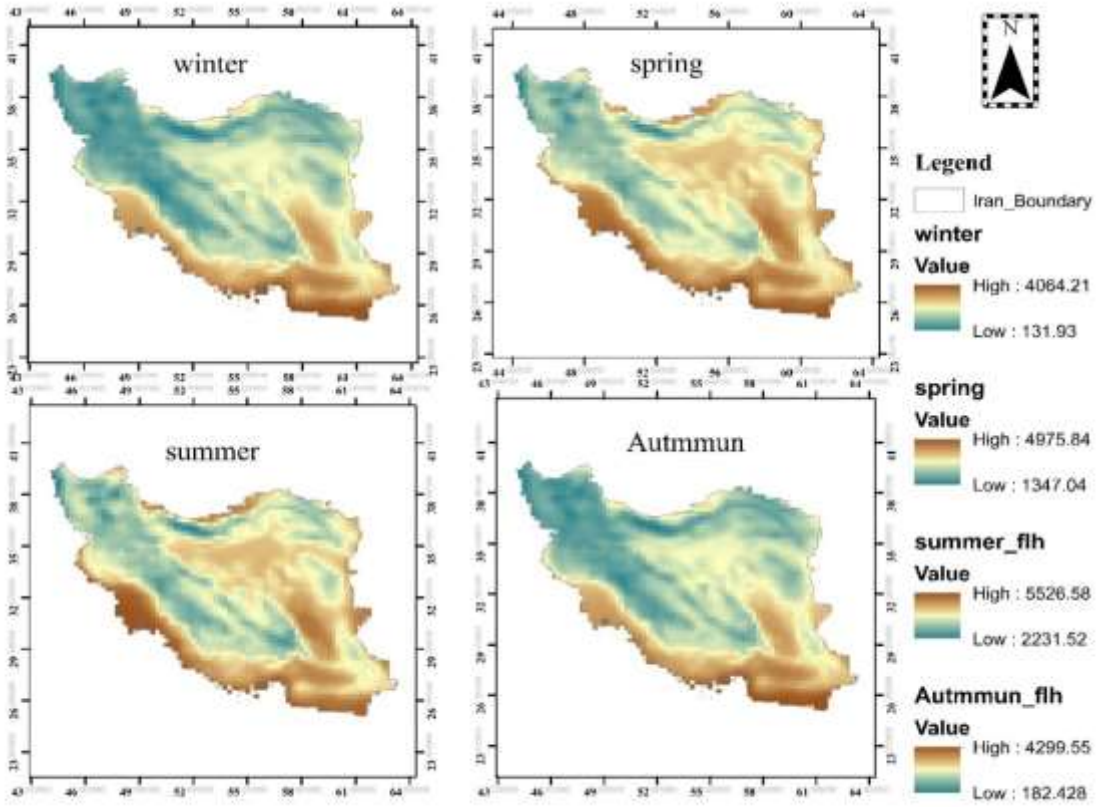

Figure 9. Raster map of seasonal FLH in Iran (1940-2023).

The annual spatial distribution pattern of freezing level height is similar to the seasonal pattern (Figure 10). The effect of longitude and latitude is significantly visible in the annual spatial pattern (Figure 11 and Table 4). In the annual pattern, the Alam-Kuh areas have the lowest average freezing level height, while Chabahar (4347.5 meters) in southeastern Iran has the highest average freezing level height (Figure 12).

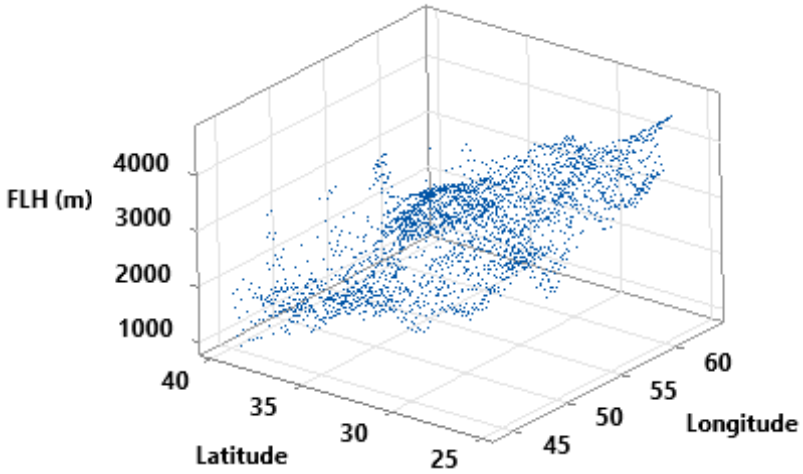

Figure 10. The pattern of spatial distribution of Annual FLH (1940-2023).

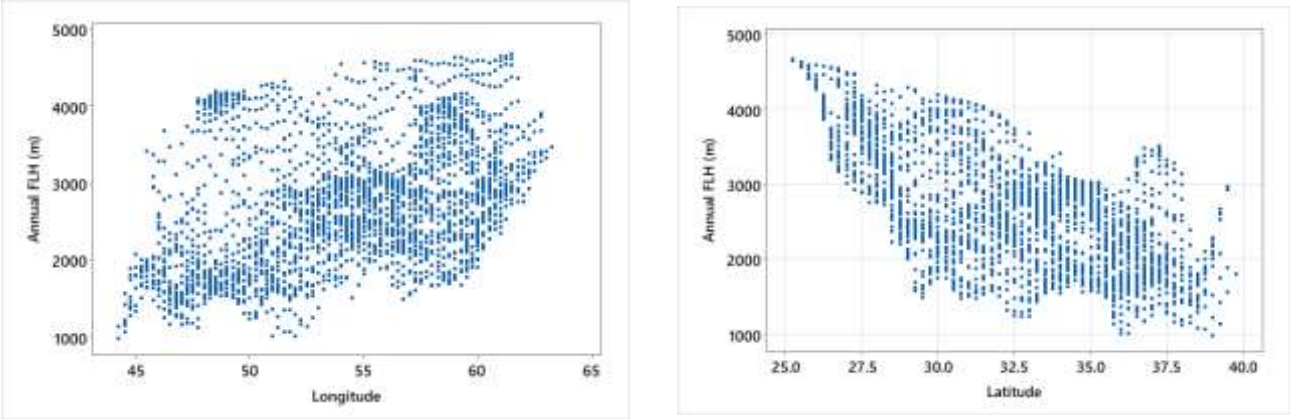

Figure 11. Spatial Distribution of Annual FLH (1940-2023) with latitude and longitude.

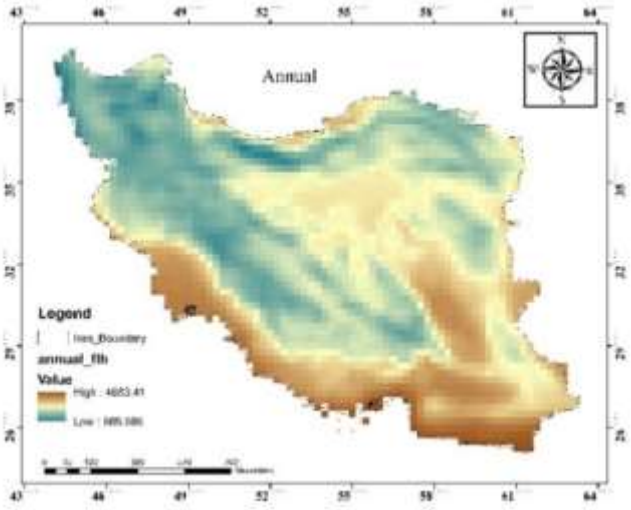

Figure 12. Annual Pattern of FLH (1940-2023)

3-5. Comparison of radiosonde data and reanalysis data

The values of FLH are data from upper atmosphere levels and cannot be measured through the network of ground-level stations. On the other hand, the very few number of upper atmosphere stations in Iran, the inadequacy and continuity of data, and the location of these stations within urban environments that act as heat islands and cannot reflect the natural conditions of freezing level height, the analysis of the trend of changes in FLH using statistical methods cannot be followed. Therefore, only a case-by-case comparison of ERA5 reanalysis data with data from the country's stations on specific days at a few upper atmosphere stations has been considered (Table 5). The results show that the data are largely consistent, especially in January and February.

Table 5. Comparison of FLH radiosonde data and reanalysis data.

ECMWF(m)	Radiosonde(m)	Station	hour	Date
1965	2225	Mehrabad	12	1/1/2020
1673	1872	Tabriz	12	1/1/2020
3712	3943	Zahedan	00	15/3/2020
2873	3050	Kermanshah	00	15/3/2017
2606	2850	Esfahan	00	15/3/2017
2401	2539	Ahwaz	00	1/1/2016
1412	1501	Esfahan	00	15/10/2021

The FLH at observation stations is slightly higher, which could be due to two factors. First, environmental effects (higher urban heat) on radiosonde. Second, Reanalysis data is the average over a spatial range that varies depending on spatial, whereas radiosonde data are recorded at specific points. Also, when the wind blows, the radiosonde's ascent path is not vertical and shows different temperature gradients at different altitudes; especially when encountering an inversion layer. In this case, comparing radiosonde data with reanalysis data is difficult. Khansalari (2020) also emphasizes that the local and point-by-point study of freezing level height is mostly the result of the passage of weather systems and synoptic conditions of the month or season, and cannot reflect the consequences of climate change.

4. Conclusion

With global warming and climate change in recent years, the study of changes in the freezing level height has attracted the attention of many atmospheric scientists. Changes in the critical zero-degree Celsius threshold can lead to changes in atmospheric circulation patterns, precipitation regimes, and the intensity of weather events.

Investigations of monthly changes in freezing level height (FLH) show that the lowest FLH value occurs in January, fluctuating from ground level (zero) to a maximum height of 4347.5 meters. The maximum freezing level height reaches 5894.1 meters in August in southeastern Iran (Chabahar). The highest coefficient of variation in FLH is observed in January (cv=12.9), due to the passage of cold weather systems over the region, while the lowest occurs in July (cv=3.6), due to the establishment of subtropical high pressure and the stability of the atmosphere during the summer months. The average FLH reaches its lowest level in winter (1576.7 meters) and its highest in summer (3924.7 meters). The maximum range of changes in the average FLH is 1049.9 meters, which is observed in the autumn. The mean annual FLH is 2733.7 meters, with a standard deviation of 139.6 meters. The average annual fluctuation of FLH is 721.6 meters (the average annual minimum FLH is 2374 meters, and the average maximum annual FLH is 3095.6 meters).

In general, the trend of temporal changes of FLH on a monthly scale shows a significant increase at the 0.5 alpha level from December to April (the cold period of the year). The highest increasing slope is observed in April. Seasonal changes in the freezing level are similar to monthly changes and follow the same trend. Seasonal variations in FLH, such as monthly, show an increasing trend during winter, spring, and autumn. The highest increasing slope was observed in winter. The freezing level height during summer does not show a significant trend. On an annual scale, the changes in the freezing level height show a significant increasing trend at the 0.01alpha level.

The spatial changes in FLH show a significant relationship with both longitude and latitude in Iran. As latitude increases, the height of the glacier surface decreases. On the other hand, with the increase in longitude, the height of FLH also increases (this issue can be caused by the weakness of vegetation and the increase in soil surface temperature in the lowland areas of southern and especially the southeastern Iran compared to the mountainous areas in the west and north of the country). The degree and intensity of the relationship between FLH and the geographical location is greater during winter months.

Given the decrease in snow cover and the increase in heavy precipitation in Iran, a long-term assessment of changes in freezing level elevation can improve the prediction of these variables, so that water resources can be managed more optimally.

References

Bradley, R.S., Keiming, F.T., Diaz, H.F., & Hardy, D.R. (2009). Recent changes in freezing level heights in the tropics with implications for the deglacierization of high mountain regions. *Geophysical Research Letters*, 36, L17701. https://doi.org/10. 1029/2009GL037712.

Chen, Z., Chen, Y., & Li, W. (2012). Response of runoff to change of atmospheric 0C level height in summer in arid region of Northwest China. *Science China Earth Sciences*, 55(9), 1533– 1544.

https://doi.org/10.1007/s11430-012-4472-6.

Coudrain, A., Francou, B., & Kundewicz, Z. W. (2005). Glacier shrinkage in the Andes and consequences for water resources. *Hydrol. Sci. J.*, 50, 925932, doi:10.1623/hysj.2005.50.6.925.

Dessens, J. (1986). Hail in southwestern France. I: Hailfall characteristics and hailstorm environment. *Journal of Climatology & Applied Meteorology*, 25, 35–47. https://doi.org/10.1175/1520-0450(1986)0252.0.CO;2.

Diaz, H.F., & Graham, N.E. (1996). Recent changes in tropical freezing heights and the role of sea surface temperature. *Nature*, 383, 152–155. https://doi.org/10.1038/383152a0.

Diaz, H.F., Bradley, R.S., & Ning, L. (2014). Climatic changes in mountain regions of the American cordillera and the tropics: historical changes and future outlook. *Arctic Antarctic & Alpine Research*, 46(4), 735–743.

Diaz, H.F., Eischeid, J.K., Duncan, C., & Bradley, R.S. (2003). Variability of freezing levels, melting season indicators, and snow cover for selected high-elevation and continental regions in the last 50 years. *Climatic Change*, 59, 33–52. https://doi.org/10.1023/A:1024460010140

Dong, Z., Qin, D., Ren, J., Li, K., & Li, Z. (2012). Variations in the equilibrium line altitude of Urumqi Glacier No.1, Tianshan Mountains, over the past 50 years. *Chinese Science Bulletin*, (57), 4776–4783. https://doi.org/10.1007/s11434-012-5524-1.

Folkins, I. (2013). The melting level stability anomaly in the tropics. *Atmos. Chem. Phys.*, 13, 11671176, doi:10.5194/acp-13-1167-2013.

Gaffen, D.J., Santer, B.D., Boyle, J.S., Christy, J.R., Graham, N.E., & Ross, R.J. (2000). Multidecadal changes in the vertical temperature structure of the tropical troposphere. *Science*, 287, 1242–1245. https://doi.org/10.1126/science.287.5456.1242.

Guo, Y., Wang, G., & Chao, Q. (2021). Climatological analysis of freezing level height over China and its implications using homogenized in-situ data. *International Journal of Climatology*. 1-18. DOI: 10.1002/joc.7260

Hamed, K.H. (2009). Exact distribution of the Mann–Kendall trend test statistic for persistent data. *Journal of Hydrology*, 365(1-2), 86–94. https://doi.org/10.1016/j.jhydrol.2008.11.024.

Hamed, K.H., &Rao, A.R. (1998). A modified Mann-Kendall Trend test for autocorrelated data, Journal of Hydrology, 204(1-4): 182–196. https://doi.org/10.1016/S0022-1694(97)00125-X.

Harris, G., Bowman, K., & Shin, D.B. (2000). Comparison of freezing-level altitudes from the NCEP reanalysis with TRMM precipitation radar bright band data. *Journal of Climate*, 13, 4137–4148. https://doi.org/10.1175/1520-0442(2000)0132.0. CO;2.

Huang, X., Wang, S., Wang, J., Li, Y., Feng, J., & Zhang, K. (2013). Spatio-temporal changes in free-air freezing level heights in Northwest China. 1960-2012. *Quaternary International*, 313 (314), 130–136. https://doi.org/10.1016/j.quaint.2013.07.200.

Kendall, M.G. (1970). *Rank Correlation Methods*, 2nd Ed., New York: Hafner.

Khansalari, S. (2020). climate change in the height of the freezing line and its synoptic analysis at the airports of Mehrabad, Mashhad and Kermanshah. *Journal of Meteorology and Atmospheric Sciences*, 3, 201-223.

Khorshiddoust. A, Rasouli. A, &Zanganeh. S. (2018) .Modeling and trending of temperature and precipitation extreme indices in Lake Urmia basin. *Natural Hazards Journal*, 7, 175-194.

Liu, X., Ma, Z., Huang, X., & Li, L. (2020). How does grazing exclusion influence plant productivity and community structure in alpine grasslands of the Qinghai-Tibetan Plateau?. *Global Ecology and Conservation*, 23, e01066. https://doi.org/10.1016/j.gecco.2020.e01066.

Lornezhad, E., Ebrahimi, H., & Rabieifar, H.R. (2023). Analysis of precipitation and drought trends by a modified Mann–Kendall method: a case study of Lorestan province, Iran. *Water Supply*, 23 (4),

1557–1570. https://doi.org/10.2166/ws.2023.068

Mann, H.B. (1945). Nonparametric tests against trend. *Econometrica*l, 13, 245-259.

Mardones, P., & Garreaud, R. D. (2020). Future changes in the free tropospheric freezing level and rainsnow limit: The case of central Chile. *Atmosphere*, 11(11), 1259. doi: 10.3390/atmos11111259

Pepin, N., Bradley, R.S., Diaz, H.F., Baraer, M., Caceres, E. B., Forsythe, N., Fowler, H., Greenwood, G., Hashmi, M. Z., Liu, X. D., Miller, J. R., Ning, l., Ohmura, A., Palazzi, E., Rangwala, I., Schoner, W., Severskiy, I., Shahgedanova, M., Wang, M. B., Williamson, S.N., & Yang, D.Q. (2015). Elevation dependent warming in mountain regions of the world. Nature Climate Change, 5, 424–430. http://doi.org/10.1038/ NCLIMATE2563

Pohlert, T. (2016). Non-parametric trend tests and change-point detection. CC BY-ND, 4, 1-18.

Seidel, D.J., & Free, M. (2003). Comparison of lower-tropospheric temperature climatologies and trends at low and high elevation radiosonde sites. *Climatic Change*, 59, 53–74. https://doi.org/10. 1023/A:1024459610680.

Sen, P. K. (1968). Estimates of the regression coefficient based on Kendall's Tau. *Journal of the American Statistical Association*, 63(324), 13791389.

Shi, P., Ma, X., Chen, X., Qu, S., & Zhang, Z. (2013). Analysis of variation trends in precipitation in an upstream catchment of the Huai River. Mathematical Problems in Engineering, Article ID: 929383.

Tabari, H., Taye, M.T. & Willems, P. (2015). Statistical assessment of precipitation trends in the upper Blue Nile River basin. *Stoch Environ Res Risk Assess*, 29, 17511761. https://doi.org/10.1007/s00477-015-1046-0

Theil, H. (1950). A rank-invariant method of linear and polynomial regression analysis. *Indagationes mathematicae*, 12(85), 173.

Vuille, M., Bradley, R. S., & Keimig, F. T., (2004). Interannual climate variability in the central Andes and its relation to tropical Pacific and Atlantic forcing. *J. Geophys. Res.*, 105(D10), 12, 44712,460, doi:10.1029/2000JD900134.

Vuille, M., Francou, B., Wagnon, P., Juen, I., Kaser, G., Mark, B. G., & Bradley, R. S. (2008). Climate change and tropical Andean glaciersPast, present and future. *Earth Sci. Rev.*, 89, 7996, doi:10.1016/j.earscirev.2008.04.002.

Wang, S., Zhang, M., Pepin, N.C., Li, Z., Sun, M., Huang, X., & Wang, Q. (2014). Recent changes in freezing level heights in high Asia and their impact on glacier changes. *Journal of Geophysical Research Atmospheres*, 119, 1753–1765. https://doi.org/ 10.1002/2013JD020490.

Zhang, G., Li, Z., Wang, W., & Wang, W. (2014a). Rapid decrease of observed mass balance in the Urumqi glacier no. 1, Tianshan Mountains, Central Asia. Quaternary International, 349(28), 135–141. https://doi.org/10.1016/j.quaint.2013.08.035.

Zhang, M., Dong, L., Wang, S., Zhao, A., Qiang, F., Sun, M., & Wang, Q. (2014b). Increasing free-air 0C isotherm height in Southwest China from 1960 to 2010. *Journal of Geographical Sciences*, 24(5), 833–844. https://doi.org/10.1007/s11442-014- 1123-1.

Zhang, Y., & Guo, Y. (2011) Variability of atmospheric freezing-level height and its impact on the cryosphere in China. *Annals of Glaciology*, 52, 81–88. https://doi.org/10.3189/172756411797252095.